

Constraint Learning to Define Trust Regions in Predictive-Model Embedded Optimization

Chenbo Shi^{*}, Mohsen Emadikhiav[†], Leonardo Lozano[‡], David Bergman[§]

October 20, 2022

Abstract

There is a recent proliferation of research on the integration of machine learning and optimization. One expansive area within this research stream is predictive-model embedded optimization, which proposes the use of pre-trained predictive models as surrogates for uncertain or highly complex objective functions. In this setting, features of the predictive models become decision variables in the optimization problem. Despite a recent surge in publications in this area, only a few papers note the importance of incorporating trust region considerations in this decision-making pipeline, i.e., enforcing solutions to be similar to the data used to train the predictive models. Without such constraints, the evaluation of the predictive model at solutions obtained from optimization cannot be trusted and the practicality of the solutions may be unreasonable. In this paper, we provide an overview of the approaches appearing in the literature to construct a trust region, and propose three alternative approaches. Our numerical evaluation highlights that trust-region constraints learned through isolation forests, one of the newly proposed approaches, outperform all previously suggested approaches, both in terms of solution quality and computational time.

Keywords: Data-driven decision making; integration of machine learning and optimization; trust region; constraint learning; isolation forest

1 Introduction

The use of pre-trained predictive models in optimization decision problems is nothing new. In this setting, the collected data includes a set of controllable independent variables as past decisions (sometimes together with uncontrollable variables) and their corresponding outcomes. Practitioners benefit by learning from data to make decisions that result in more favorable outcomes [Biggs et al., 2017, Mišić, 2020] through surrogate models, to learn the underlying relationship between the controllable independent variables and their outcome [Biggs et al., 2017, Grimstad and Andersson, 2019a]. Once the relationship is learned, one can solve an optimization problem defined over the predictive model, where decision variables in the optimization problem correspond to the controllable independent variables, and the objective function is given by the outcome of the pre-trained predictive model. We will refer to this decision-making paradigm as *predictive-model embedded optimization* (PMO).

^{*}Department of Operations and Information Management, School of Business, University of Connecticut, chenbo.shi@uconn.edu

[†]Department of Information Technology and Operations Management, Florida Atlantic University, memadikhiav@fau.edu

[‡]Department of Operations, Business Analytics, and Information Systems, University of Cincinnati, leolozano@uc.edu

[§]Department of Operations and Information Management, School of Business, University of Connecticut, david.bergman@uconn.edu

Examples abound; consider a traditional setting in advertising. Suppose a retailer can select from among n advertising channels. Given a budget of B dollars, how much should the retailer allocate to each advertising channel to maximize revenue? Classical Operations Research methods suggest that a predictive model such as regression model can be fit on historical data (including both previous decisions, market conditions, and revenue) to predict revenue, and then the allocation decision variables can be selected to maximize predicted revenue. Depending on the predictive model chosen, the optimization model can be appropriately formulated. For example, if the predictive model chosen is a linear regression, the optimization problem can be modeled as a linear programming model; if the predictive model chosen is a neural network or a random forest, recent research shows how a mixed-integer model can be formulated (for instance, Anderson et al. [2020]).

Because of its generality, PMO finds potential applications throughout the analytical landscape. There is a major issue with the real-world application of PMO, which practitioners are well aware of: decisions produced by PMO are often unrealistic because they can be very different from what is observed historically in data. This happens because often the existing PMO frameworks ignore the *trust region*, i.e., ensuring that solutions to the optimization problem are similar to the data used to train the predictive models [Maragno et al., 2021, Mistry et al., 2021, Schweidtmann et al., 2022].

Let us demonstrate this issue using an example in a wine production context on a dataset that has been used before in the PMO literature [Mišić, 2020, Wang et al., 2021]. Wine scores are typically used by critics to specify their opinion about wine quality. Suppose a wine producer is equipped with a dataset that includes physicochemical property measurements of varieties of wine as features (e.g., pH, fixed acidity, residual sugar, etc.) along with the corresponding wine scores. The producer wants to leverage this dataset and build a PMO model to determine the best combination of physicochemical property measurements that maximizes the expected wine score.

Figure 1 shows a scatter plot (pH versus fixed acidity) for two solutions obtained via a PMO model defined over a trained neural network (which is one of the most popular predictive models nowadays) and historical observations in the data (features are scaled between 0 and 1). The first solution is obtained by solving the corresponding optimization model without additional constraints (represented by an orange cross) and the second solution is obtained by incorporating trust-region constraints (represented by a blue diamond). Measurements of pH and fixed acidity in historical observations present a negative correlation, which is expected as higher acidity should correspond with a lower pH. The initial solution obtained, however, completely violates this relationship, rendering the solution unacceptable. Alternatively, the second solution is closer to the training data and aligns with the aforementioned chemical considerations. It may be argued that the predictive model is not good enough to capture the inverse correlation. However, in predictive modeling applications, a predictive model is usually selected based on its overall predictive performance instead of considering such specific correlation relationships between pairs of features. By solving an optimization problem defined over such a predictive model, we cannot guarantee that the solution obey the practical requirements. In fact, it is a common character of solutions of PMOs falling at the extremes of the feasible region [Maragno et al., 2021].

The example above highlights how the solutions obtained by PMO can be inappropriate for a particular application. That is not the only potential issue. Even if a wine could be created that has the relationship of high acidity and high pH, the evaluation of the objective function of the pre-trained model at that point would be untrustworthy. If the optimization problem selects a solution that is too different from the training data of the predictive model, one cannot trust the prediction produced by the predictive model at that point (i.e., the error is immeasurable). This is well known in the application of predictive modeling, where it is common to assume that the unobserved/test data comes from the same distribution as the historical/training data.

There are therefore two major issues with a direct application of PMO as presented thus far in this paper: (1) the solutions can be inappropriate for the application, and (2) the validity of the predictive model at the solution obtained could be untrustworthy. To address these issues, constraints can be added for each possible application to ensure that the decisions model physical or other real-world considerations, but these relationships might be highly non-linear, or perhaps unknown to the modeler. One might also try to examine all pairs of variables and make sure they are reasonably correlated as desired, but this can be challenging to identify for higher degree relationships and can lead to over constraining.

Recently, some research has focused on developing methods to incorporate trust region in PMOs. For instance, Biggs et al. [2017] and Maragno et al. [2021] use the convex-hull of observations in the dataset to

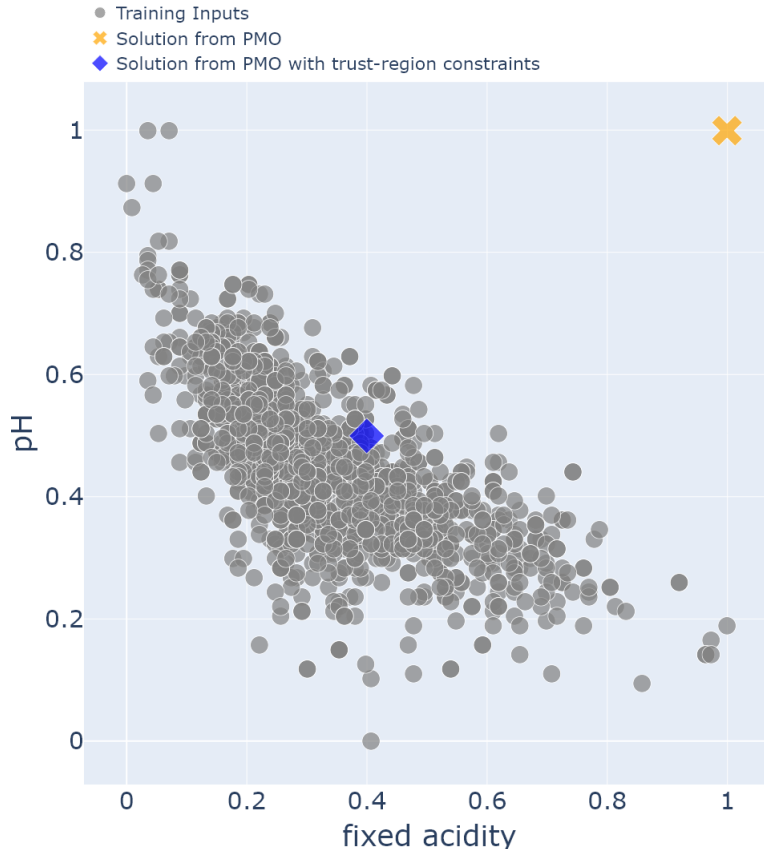


Figure 1: A scatter plot comprising two variables (pH and fixed acidity) for two solutions from a PMO model

model a trust region, while Schweidtmann et al. [2022] utilize a one-class support vector machine (SVM) to determine constraints for the trust region. In essence, constructing a trust region for PMOs ensures that the solutions are not outliers compared to the historical observations. In this paper, we provide an overview of the existing methods for modeling the trust region in PMOs and explore three additional ways to detect outliers, which are melded into PMOs as a trust region: the first defines a trust region by selecting queries from a pre-trained *isolation forest* [Liu et al., 2008]; the second uses *Mahalanobis distance* [Mahalanobis, 1936] to constrain the solutions within a given distance of the training data, which is particularly useful when an assumption on multivariate normality is reasonable; and the third incorporates constraints to ensure that the solution is within a limited distance of K -nearest neighbors [Altman, 1992] in the training data.

We design computational experiments to compare the performance of our proposed trust-region constraints to the existing approaches in the literature. To our knowledge we are the first to evaluate different trust regions against each other both in terms of solution quality and computational performance (measured in solution resolution time). For our experiments, we generate a testbed of problem instances based on 7 different benchmark functions and use multiple predictive models to fit the training data within our PMO approach. Our results indicate that our proposed constraints compare favorably with the existing approaches from the literature, particularly our Isolation-Forest constraints.

Our contributions are therefore as follows:

1. Although researchers have independently developed methods for modeling the trust region in PMOs, to our best knowledge, we are the first to provide a comparison of existing methods in terms of solution quality and CPU time.
2. We propose three alternative methods for modeling the trust region in PMOs. Our results show the

effectiveness of our proposed approaches, particularly the trust region defined by Isolation Forest, compared to existing ones in the literature both in terms of solution quality and computational times.

3. We present a set of benchmark instances that can be used by the optimization community for further research on related topics.

2 Literature Review

Multiple works from the literature consider optimization problems defined over trained predictive models, ranging from simple linear regressions to more complex predictive models such as random forest and neural networks. Bertsimas et al. [2016] optimize over an estimated ridge regression model seeking to improve the efficacy of chemotherapy regimens in clinical trials. Huang et al. [2019] and Baardman et al. [2019] propose optimization models defined over linear regressions in the context of retailers location decisions and scheduling of promotion vehicles, respectively. Ferreira et al. [2016] use random forest to estimate the demand of a product based on its price, and develop an optimization model over a trained random forest to determine product prices that maximize total expected revenue. Other application areas include food delivery Liu et al. [2020], scholarship allocation Bergman et al. [2022], personalized pricing Biggs et al. [2021], and auctions Verwer et al. [2017].

Optimization problems defined over trained predictive models are often challenging to solve, depending on the properties of the underlying predictive model. Mišić [2020] and Biggs et al. [2017] propose exact solution approaches for optimization problems defined over tree ensembles. Mixed integer programming (MIP) formulations for optimization models defined over trained neural networks are studied by Cheng et al. [2017], Fischetti and Jo [2018], Bunel et al. [2018], Dutta et al. [2018], Bergman et al. [2022], Grimstad and Andersson [2019a], Schweidtmann and Mitsos [2019], Tjeng et al. [2019], Grimstad and Andersson [2019b], Botoeva et al. [2020], Anderson et al. [2020] and Tsay et al. [2021]. Ensembles of neural networks are studied by Wang et al. [2021]. A closely related research area deals with so-called *verification problems*, which seek to verify relationships between the inputs and outputs of neural networks, as well as to measure the sensitivity of the outputs to small changes in the inputs. These problems are often formulated as mixed-integer programs defined over trained neural networks [Lomuscio and Maganti, 2017, Cheng et al., 2017, Katz et al., 2017, Serra et al., 2018].

In predictive modeling, it is common to assume that the unobserved/test data comes from the same distribution as the historical/training data, which is used to build predictive models [Amodei et al., 2016], otherwise the predictive models' applicability would be limited. Similarly, a solution obtained via PMO can be seen as a new observation in the dataset. The prediction provided by the predictive model should only be trusted if the solution comes from the same distribution as the training data. To constrain the predictive models from extrapolating, a few recent studies have considered the notion of trust region in PMOs. Teixeira et al. [2006] use a clustering technique to define a trust region of a nonparametric input space where the predictions of the predictive model are reliable. Biggs et al. [2017] and Maragno et al. [2021] define a similar subspace using the convex hull of observations in the training data to model a trust region by constraining PMO solutions to be within this convex hull. Mistry et al. [2021] add a penalty term to the objective function so that solutions that lie far away from the subspace constructed by principle component analysis (PCA), are penalized. Schweidtmann et al. [2022] constrain the solutions to belong to a validity domain defined by a pre-trained one-class SVM, a classifier for outlier detection.

3 PMO with Trust-Region Constraints

We consider a trained predictive model that is established to learn the relationship between a dependent variable y and a vector of independent variables $\mathbf{x} = \{x_1, \dots, x_n\}$ based upon a set of historical observations $\mathcal{S} = \{(\hat{\mathbf{x}}^j, \hat{y}^j)\}_{j=1}^q$. We refer to set $\mathcal{S}^x = \{\hat{\mathbf{x}}^j\}_{j=1}^q$ as the training input data of the problem and refer to the components of vector \mathbf{x} as features with index set given by $\mathcal{I} = \{1, \dots, n\}$. For simplicity, we assume that all the independent variables are continuous and each independent variable is scaled to $[0, 1]$. We define decision variables \mathbf{x} to determine the value of each independent variable and let the predicted outcome of

the predictive model be given by $F(\mathbf{x})$. We study problems of the following form:

$$\min_{\mathbf{x}} F(\mathbf{x}) \tag{1a}$$

$$\text{s.t. } \mathbf{x} \in [\mathbf{0}, \mathbf{1}]. \tag{1b}$$

We consider three different predictive models associated with function $F(\mathbf{x})$: linear regression (LR), random forest (RF), and neural networks (NN). The mathematical formulations corresponding to each one of the three predictive models are discussed in Appendix A. Constraints are then added to the model above to ensure that solutions found are within a trust region. In Section 3.1 we first review three existing types of trust region constraints from the literature. We then introduce our proposed constraints in Section 3.2.

3.1 Overview of the Existing Trust-Region Constraints

3.1.1 Convex Hull Constraints

Maragno et al. [2021] characterize a trust region using the convex hull (CH) of the training input data \mathcal{S}^x , which is the smallest convex polytope that contains all the points in \mathcal{S}^x . For each sample point $\hat{\mathbf{x}}^j$ in \mathcal{S}^x , an auxiliary decision variable w_j is added to describe the convex hull. Let $\mathcal{J} = \{1, \dots, q\}$ be the index set of \mathcal{S}^x . The trust region is then represented by the following constraints:

$$\mathbf{x} = \sum_{j \in \mathcal{J}} w_j \hat{\mathbf{x}}^j \tag{2a}$$

$$\sum_{j \in \mathcal{J}} w_j = 1 \tag{2b}$$

$$w_j \geq 0 \quad \forall j \in \mathcal{J}, \tag{2c}$$

which ensure that any PMO solution belongs to the convex hull of the training input data.

3.1.2 One-Class SVM Constraints

One-class SVM is an unsupervised machine learning algorithm that specifies a boundary to classify sample points for outlier detection. In other words, if a sample point falls outside of the boundary learned through one-class SVM, it is classified as an outlier. The boundary is mathematically represented using a *decision function* which may take various forms. The form of the decision function depends on the type of *kernel function* used to model the data. In SVMs, a kernel is a function that is used to transform the data into higher dimensions so that data points can be linearly separable [Hofmann et al., 2008]. Depending on the complexity of the data, different kernel functions such as linear, polynomial, and Gaussian, among others may be used. It has been shown that complex boundaries can be accurately modeled using a Gaussian radial basis kernel [Tax, 2001]. Let $I_{SV} \subseteq \mathcal{S}^x$ denote the set of support vectors from the training input data. A decision function based on a Gaussian radial basis kernel is:

$$\sum_{j \in I_{SV}} \alpha_j \exp(-\gamma \|\hat{\mathbf{x}}^j - \mathbf{x}\|^2) - \rho, \tag{3}$$

where hyper-parameter γ is tuned before the training process, while parameters α and ρ are learned during the training process for one-class SVMs [Schölkopf et al., 1999].

Schweidtmann et al. [2022] propose trust-region constraints based on one-class SVM classifiers as the ones described above. These constraints ensure that PMO solutions \mathbf{x} fall inside a trust region and are modeled as:

$$\sum_{j \in I_{SV}} \alpha_j \exp(-\gamma \|\hat{\mathbf{x}}^j - \mathbf{x}\|^2) \geq \rho, \tag{4}$$

which ensure that solutions \mathbf{x} are not classified as outliers by the pre-trained one-class SVM classifier.

PMO models with trust region SVM constraints (4) can be solved directly with off-the-shelf mixed-integer non-linear programming solvers such as BARON [Sahinidis, 2017]. To boost the running time performance of this model, we alternatively propose a heuristic branch-and-cut algorithm that enforces trust-region SVM constraints (4) dynamically by checking if PMO solutions violate these constraints via callbacks. Our experiments show that even if the branch-and-cut algorithm is not able to prove optimality, it is able to find high quality solutions quickly. We present the details of this heuristic algorithm in Appendix section B.

3.1.3 Principal Component Analysis Constraints

Mistry et al. [2021] incorporate the trust region into PMOs by penalizing solutions that are far away from the training input data. To fulfill this idea, they first define a subspace of the training input data that is created using principal component analysis [Jolliffe, 2002] and then include a convex penalty term to penalize the objective function based on the solution’s distance to the defined subspace.

Specifically, given a training input data \mathcal{S}^x with n features, PCA defines a set of n ordered and orthogonal principal components, $\Phi = [\phi_1 \dots \phi_n]$. Among all the n principal components, oftentimes the top k (such that $k < n$) principal components, $\Phi' = [\phi_1 \dots \phi_k]$, are able to explain most of the variance in \mathcal{S}^x . The resulting subspace of \mathcal{S}^x is a vector denoted by (ϕ_1, \dots, ϕ_k) . Mistry et al. [2021] use the following penalty term to penalize the solutions \mathbf{x} that are far away from the desired subspace:

$$\text{cvx}_\lambda(\mathbf{x}) = \lambda \| (\mathbf{I} - \Phi' \Phi'^T) \text{diag}(\boldsymbol{\sigma})^{-1} (\mathbf{x} - \boldsymbol{\mu}) \|_2^2, \quad (5)$$

where λ is a non-negative penalty parameter, \mathbf{I} is the identity matrix, $\boldsymbol{\mu}$ is the sample mean and $\boldsymbol{\sigma}$ is the sample standard deviation. Note that PCA is calculated with standardized \mathcal{S}^x since it is sensitive to scaling, and \mathbf{x} is standardized using $(\boldsymbol{\sigma})^{-1} (\mathbf{x} - \boldsymbol{\mu})$ so that \mathbf{x} and PCA are in the same scale.

In order to compare Mistry et al. [2021] penalty method of enforcing a trust region with the other constraint-based approaches surveyed, we model the trust region given by PCA with the following constraint:

$$\| (\mathbf{I} - \Phi' \Phi'^T) \text{diag}(\boldsymbol{\sigma})^{-1} (\mathbf{x} - \boldsymbol{\mu}) \|_2^2 \leq \gamma, \quad (6)$$

where threshold γ is a parameter that controls the looseness (tightness) of the constraint.

3.2 Our Proposed Trust-Region Constraints

We propose three types of trust-region constraints based on three additional techniques used to identify outliers.

3.2.1 Isolation Forest Constraints

Our first proposed type of trust region constraints are originated from a pre-trained isolation forest classifier [Liu et al., 2008], which is a model used for outlier (anomaly) detection.

An isolation forest is an ensemble of *isolation trees* where each isolation tree is trained over a randomly selected subsample of the training data. An isolation tree is a model that detects outliers using independent variables \mathbf{x} by checking a series of *splits*. A split specifies a condition on a single feature $i \in \mathcal{I}$ using a query of the form “Is $x_i \leq a$?”, where a is a random value within the domain of feature i . The series of splits arrange a tree, with each split node branching into two child nodes. To determine whether a data point is an outlier, we start from the root node of the tree and recursively check the query of each split node. If the condition is true, the data point is assigned to the left branch of the split node, otherwise it is assigned to the right branch of the split node. The data point eventually is assigned to a *leaf node*, for which there are no more splits.

An isolation tree uses a predetermined threshold, d , associated with the depth of the leaf nodes. Data points that are assigned to leaf nodes with depth smaller than or equal to d are classified as outliers. Figure

2 illustrates an example of an isolation forest classifier having $d = 2$. Leaf nodes with depth smaller than or equal to 2 correspond to data points that are classified as outliers, while leaf nodes with depth larger than 2 correspond to data points that are classified as inliers.

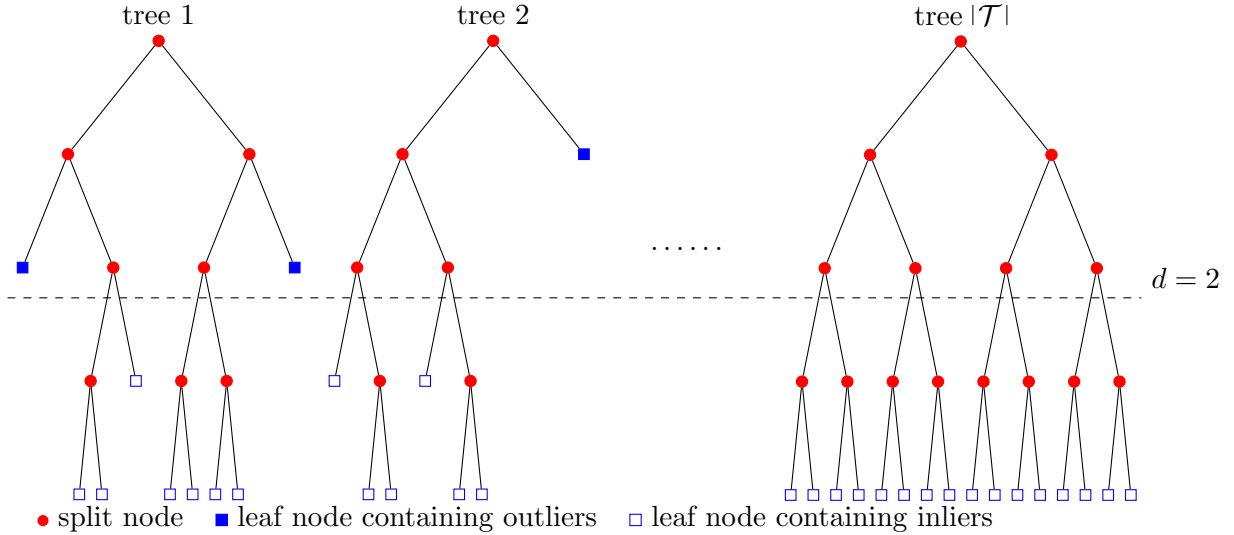


Figure 2: Illustration of an isolation forest with threshold $d = 2$

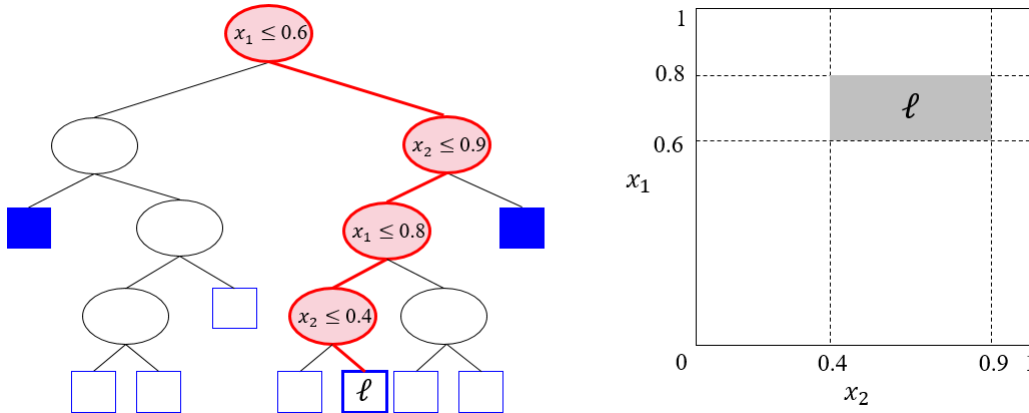


Figure 3: Left: tree 1 from Figure 2, where the shaded split nodes and bold edges indicate how a solution that fulfills the queries in those split nodes falls into leaf node ℓ . Right: corresponding domain of leaf node ℓ , e.g., the lower bound in the dimension of feature 2 of leaf node ℓ from tree 1 is $l_{2,1,\ell} = 0.4$.

We propose trust-region constraints to ensure that solutions \mathbf{x} are not classified as outliers by a pre-trained isolation forest. The goal of these constraints obtained from an isolation forest is to ensure that PMO solutions do not correspond to any leaf node with a shallow depth, i.e., a depth less than or equal to d . We remark that any solution vector \mathbf{x} corresponds to exactly one leaf node in each isolation tree and because there is a unique path between the root node of a tree and each leaf node, then leaf nodes correspond to a series of lower and upper bounds on the variable features, given by the queries associated with split nodes in the path from the root node. Figure 3 illustrates the relationship between paths in an isolation forest and variable features bounds. We exploit these bounds to formulate our trust-region constraints as follows.

Consider an isolation forest with $|\mathcal{T}|$ isolation trees. Let \mathcal{L}_t be the set of leaf nodes in tree $t \in \mathcal{T}$. We introduce binary decision variable $y_{t,\ell}$ that takes a value of 1 if leaf node $\ell \in \mathcal{L}_t$ from tree $t \in \mathcal{T}$ is selected.

We introduce auxiliary decision variables z_i^{LB} and z_i^{UB} to specify the range of each variable feature $i \in \mathcal{I}$. We denote the depth of leaf nodes by $\delta(t, \ell)$, and let the lower and upper bounds corresponding to a leaf node be $l_{i,t,\ell}$ and $u_{i,t,\ell}$ for all $i \in \mathcal{I}$, $t \in \mathcal{T}$, and $\ell \in \mathcal{L}_t$. Our proposed isolation-forest constraints are:

$$\sum_{\ell \in \mathcal{L}_t} y_{t,\ell} = 1 \quad \forall t \in \mathcal{T} \quad (7a)$$

$$y_{t,\ell} = 0 \quad \forall t \in \mathcal{T}, \ell \in \mathcal{L}_t \mid \delta(t, \ell) \leq d \quad (7b)$$

$$\sum_{\ell \in \mathcal{L}_t} l_{i,t,\ell} y_{t,\ell} \leq z_i^{LB} \quad \forall t \in \mathcal{T}, \forall i \in \mathcal{I} \quad (7c)$$

$$1 - \sum_{\ell \in \mathcal{L}_t} (1 - u_{i,t,\ell}) y_{t,\ell} \geq z_i^{UB} \quad \forall t \in \mathcal{T}, \forall i \in \mathcal{I} \quad (7d)$$

$$z_i^{LB} \leq x_i \leq z_i^{UB} - \epsilon \quad \forall i \in \mathcal{I} \quad (7e)$$

$$z_i^{LB}, z_i^{UB} \in [0, 1] \quad \forall i \in \mathcal{I} \quad (7f)$$

$$y_{t,\ell} \in \{0, 1\} \quad \forall t \in \mathcal{T}, \ell \in \mathcal{L}_t \quad (7g)$$

Constraints (7a) ensure that exactly one of the leaf nodes from each tree in the isolation forest is selected. Constraints (7b) require that the depth of the selected leaf node l in each tree t is larger than the threshold d . Constraints (7c) and constraints (7d) ensure that, for any leaf node that is selected, the domain of the solution is limited to the feature ranges determined by the path leading to that leaf node. Constraints (7e) ensure that \mathbf{x} belongs to the domain defined by the corresponding leaf nodes selected. The combination of these constraints ensure that solution \mathbf{x} does not correspond to a leaf node of any tree that can be labeled as an outlier.

3.2.2 Mahalanobis Distance Constraints

In Section 3.1.3, we introduced a distance-based approach to penalizing solutions further away from the training data subspace defined by PCA. Instead of capturing the distance from a data point to a subspace, we propose to use the Mahalanobis Distance (MD) [Mahalanobis, 1936], which measures the number of standard deviations between a given point and the centroid of a distribution. MD has been used for detecting multivariate outliers in different application areas such as psychology [Leys et al., 2018], archaeology [Papageorgiou, 2020], and geotechnics [Zheng et al., 2021].

We propose a MD constraint that restricts the MD between the solution \mathbf{x} and the training input data to be less than or equal to a parameter γ . Let $\Gamma(\mathbf{x})$ be the MD measure mentioned above, which is calculated as:

$$\Gamma(\mathbf{x}) = \sqrt{(\mathbf{x} - \boldsymbol{\mu})^\top \mathbf{C}^{-1} (\mathbf{x} - \boldsymbol{\mu})}, \quad (8)$$

where $\boldsymbol{\mu}$ and \mathbf{C} denote the mean vector and the covariance matrix of the training inputs, respectively. We propose adding constraint

$$\Gamma(\mathbf{x}) \leq \gamma \quad (9)$$

as a way of modeling the trust region. We remark that for implementation purposes, the squared form of function Γ can be directly inserted into the model and solved via off-the-shelf optimization solvers such as Gurobi [Gurobi Optimization LLC, 2020].

Parameter γ controls the level of conservativeness of the model. Low values for γ result in a smaller feasible region in which the solution to the optimization problem must be close to the training input data. Larger values for γ allow the outcome for the optimization model to be farther away from the training distribution. If the training input data follows a multivariate normal distribution, then $\Gamma^2(x)$ follows a chi-square distribution with n degrees of freedom, where n equals the number of dimensions of the training inputs [Johnson et al., 2014]. In practice, a point $\hat{\mathbf{x}}$ is commonly labeled as a multivariate outlier if $\Gamma^2(\hat{\mathbf{x}})$ exceeds a chi-square critical value with n degrees of freedom at significance level α in $\{0.05, 0.01, 0.001\}$. As

a result, if the training input data follows a multivariate normal distribution, then a natural value for γ is given by $\gamma = \sqrt{\chi_{n,1-\alpha}^2}$. We remark that in settings in which the training inputs do not follow a multivariate distribution, constraints based on MD can still be useful after tuning the value of γ .

3.2.3 K-Nearest Neighbors Constraints

Our third class of constraints considers the distance between the solution of the optimization model and the K closest points from the input data, denoted as its K -nearest neighbors. This is a straightforward way to ensure that the solution is less likely to be labeled as an outlier as the solution will be close to the input data. This type of measures have been widely used for classification and regression problems [Friedman, 2017]. Among the multiple measures of distance available, we propose a formulation that considers the ℓ^1 -norm distance metric, which computes the sum of the absolute difference of the individual components of the vectors.

Consider a training data set \mathcal{S}^x composed of q observations $\hat{\mathbf{x}}^j \in \mathbb{R}^n$ for $j \in \mathcal{J}$ (where $\mathcal{J} = \{1, \dots, q\}$ is the index set of the observations). We propose a mixed-integer linear formulation that incorporates a constraint that limits the average distance between the solution of the optimization model and its K -nearest neighbors to be less than or equal to a parameter γ . For all $i \in \mathcal{I}$ and $j \in \mathcal{J}$, let auxiliary decision variables d_{ij}^- and d_{ij}^+ capture the deviation between the i^{th} component of solution vector \mathbf{x} and the i^{th} component of sample point $\hat{\mathbf{x}}^j$. Let auxiliary decision variables w_j represent the ℓ^1 distance between \mathbf{x} and sample point $\hat{\mathbf{x}}^j$. We introduce auxiliary binary decision variables π_{kj} that take a value of 1 if sample point $\hat{\mathbf{x}}^j$ is one of the k^{th} nearest neighbors of solution vector \mathbf{x} , and auxiliary variables z_k to capture the ℓ^1 distance between \mathbf{x} and the k^{th} nearest point in \mathcal{S} (for example, z_1 captures the distance between \mathbf{x} and the closest sample point, z_2 captures the distance between \mathbf{x} and the second closest sample point, and so forth). Our proposed formulation of KNN constraints is given by:

$$x_i + d_{ij}^+ - d_{ij}^- = \hat{x}_i^j \quad \forall i \in \mathcal{I}, j \in \mathcal{J} \quad (10a)$$

$$w_j = \sum_{i \in \mathcal{I}} d_{ij}^+ + d_{ij}^- \quad \forall j \in \mathcal{J} \quad (10b)$$

$$z_k \geq w_j - M(1 - \pi_{kj}) \quad \forall j \in \mathcal{J}, k \in \{1, \dots, K\} \quad (10c)$$

$$\sum_{j \in \mathcal{J}} \pi_{kj} = k \quad \forall k \in \{1, \dots, K\} \quad (10d)$$

$$\frac{1}{K} \sum_{k \in \{1, \dots, K\}} z_k \leq \gamma \quad (10e)$$

$$\pi_{kj} \in \{0, 1\} \quad \forall j \in \mathcal{J}, k \in \{1, \dots, K\} \quad (10f)$$

$$d_{ij}^+, d_{ij}^- \geq 0 \quad \forall i \in \mathcal{I}, j \in \mathcal{J} \quad (10g)$$

$$w_j \geq 0 \quad \forall j \in \mathcal{J} \quad (10h)$$

$$z_k \geq 0 \quad \forall k \in \{1, \dots, K\} \quad (10i)$$

where M is a sufficiently large constant. Constraints (10a)–(10b) define the w -variables, while constraints (10c)–(10d) define the z -variables. Note that for $k = 1$, exactly one π_{1j} variable equals 1 and so exactly one constraint (10c) is activated, ensuring that at optimality z_1 equals the distance between \mathbf{x} and the closest sample point. For $k = 2$, then exactly two π_{2j} variables take a value of 1, activating two constraints (10c). As a result, z_2 must be greater than or equal to two of the distances between \mathbf{x} and the sample points, captured by the w -variables. At optimality, z_2 will be exactly equal to the distance between \mathbf{x} and the second closest point in the sample. The model follows the same logic for the remaining values of k . Finally, constraint (10e) ensures that the average distance to the K -nearest neighbors is less than or equal to threshold γ .

It can be seen that the size of the PMO model with KNN constraints, both in number of decision variables and constraints, grows with the size of the training data (similar to constraints using convex hull of the dataset). Hence, for large data sets solving these models would be challenging for commercial mixed-

integer programming solvers. As a heuristic approach, one may only consider the top $\beta\%$ of the training data when incorporating KNN constraints.

4 Experiments

In order to test the effectiveness of the various approaches, we evaluate the solution quality obtained by solving PMO on a variety of functions with different trust region definitions. Specifically, we utilize standard global optimization functions for which the optimal solution is known to create synthetic datasets. For each function, we randomly sample inputs from multivariate normal distributions to create a training set. For each input in the training set, we evaluate the known function (with noise), and use that to train models to predict the outcome. We can then solve a PMO with the various trust-region constraints.

This allows for a controlled experimental evaluation of the efficacy of each trust region approach. Because we know the optimal value and we can generate a data set for training predictive models, the gap between the solution value obtained via PMO and the optimal value can be calculated easily and compared across the various approaches. Furthermore, we can also compare the best point in the training data with the values obtained through PMO to see if our proposed approaches improve upon the simple best-in-sample solution. Finally, we can also provide an analysis of the solution time to see which trust-region constraints provide the smallest computational burden.

We present two sets of experimental results on two synthetic datasets based on seven global optimization benchmark functions. Given a synthetic dataset generated from a global optimization benchmark function $f(\mathbf{x})$, we first estimate the relationship (which we denote by $F(\mathbf{x})$ as in the definition of PMO) between the independent variables (i.e., the decision variables in the optimization problem) and the dependent variable using predictive modeling, then solve the PMO model, record its solution as \mathbf{x}^* , and calculate the true objective value at the solution $f(\mathbf{x}^*)$. We evaluate the quality of a solution by calculating the *true outcome* of the solution (i.e., $f(\mathbf{x}^*)$), and the *optimality error* at the optimal solution (calculated as $\Delta = |F(\mathbf{x}^*) - f(\mathbf{x}^*)|$). Note that we do not report percent optimality gaps because some of the functions have zero and/or negative evaluations at solutions.

All predictive models are trained in Python using the **scikit-learn** package [Pedregosa et al., 2011], and all optimization models are solved with Gurobi 9.0 [Gurobi Optimization LLC, 2020] in Windows 10 on an Intel(R) Xeon(R) Gold 6130 CPU @ 2.10GHz processor with 32 GB RAM.

4.1 Data Generation

We consider seven benchmark functions:

1. **Beale:** $f(\mathbf{x}) = (1.5 - x_1 + x_1x_2)^2 + (2.25 - x_1 + x_1x_2^2)^2 + (2.625 - x_1 + x_1x_2^3)^2$. The global minimum is located at $\mathbf{x}_{\min} = (3, 0.5)$, $f(\mathbf{x}_{\min}) = 0$.
2. **Peaks:** $f(\mathbf{x}) = 3(1-x_1)^2e^{-x_1^2-(x_2+1)^2} - 10(\frac{x_1}{5} - x_1^3 - x_2^5)e^{-x_1^2-x_2^2} - \frac{1}{3}e^{-(x_1+1)^2-x_2^2}$. The global minimum is located at $\mathbf{x}_{\min} = (0.23, -1.63)$, $f(\mathbf{x}_{\min}) = -6.55$.
3. **Griewank:** $f(\mathbf{x}) = \sum_{i=1}^4 \frac{x_i^2}{4000} - \prod_{i=1}^4 \cos\left(\frac{x_i}{\sqrt{i+1}}\right) + 1$. The global minimum is located at $\mathbf{x}_{\min} = (0, 0, 0, 0)$, $f(\mathbf{x}_{\min}) = 0$.
4. **Powell:** $f(\mathbf{x}) = (x_1 + 10x_2)^2 + 5(x_3 - x_4)^2 + (x_2 - 2x_3)^4 + 10(x_1 - x_4)^4$. The global minimum is located at $\mathbf{x}_{\min} = (0, 0, 0, 0)$, $f(\mathbf{x}_{\min}) = 0$.
5. **Quintic:** $f(\mathbf{x}) = \sum_{i=1}^5 |x_i^5 - 3x_i^4 + 4x_i^3 + 2x_i^2 - 10x_i - 4|$. The global minimum is located at $\mathbf{x}_{\min} = (-1, -1, -1, -1, -1)$ or $(2, 2, 2, 2, 2)$, $f(\mathbf{x}_{\min}) = 0$.
6. **Qing:** $f(\mathbf{x}) = \sum_{i=1}^8 (x_i^2 - i)^2$. The global minimum is located at $\mathbf{x}_{\min} = (1, \sqrt{2}, \sqrt{3}, \sqrt{4}, \sqrt{5}, \sqrt{6}, \sqrt{7}, \sqrt{8})$, $f(\mathbf{x}_{\min}) = 0$.
7. **Rastrigin:** $f(\mathbf{x}) = \sum_{i=1}^{10} [x_i^2 - 10 \cos(2\pi x_i)]$. The global minimum is located at $\mathbf{x}_{\min} = (0, 0, 0, 0, 0, 0, 0, 0, 0, 0)$, $f(\mathbf{x}_{\min}) = 0$.

Beale, **Griewank**, **Powell**, **Rastrigin**, **Qing**, and **Quintic** [Gavana, 2022] are commonly used for evaluating global optimization algorithms, and **Peaks** is a test function in Matlab [The MathWorks Inc, 2010].

For each function, we generate points to be used as training data for estimating the relationship $f(\mathbf{x})$ by sampling 1000 points from a multivariate normal distribution, with mean located at the global minimum point (i.e., $(3, 0.5)$ for **Beale**, $(0.23, -1.63)$ for **Peaks**, $(0, 0, 0, 0)$ for **Griewank**, $(0, 0, 0, 0)$ for **Powell**, $(2, 2, 2, 2)$ for **Quintic**, $(1, \sqrt{2}, \sqrt{3}, \sqrt{4}, \sqrt{5}, \sqrt{6}, \sqrt{7}, \sqrt{8})$ for **Qing**, and $(0, 0, 0, 0, 0, 0, 0, 0, 0, 0)$ for **Rastrigin**) and a covariance matrix randomly generated using function `make_spd_matrix` in **scikit-learn**. The outcome of each sampled point is the evaluation of the benchmark function, plus randomly generated noise (i.e., $y(\mathbf{x}) = f(\mathbf{x}) + \epsilon$). For each point, the noise ϵ is drawn from a zero-mean normal random variable with variance given by a constant $\sigma_{f(\mathbf{x})}$, where $\sigma_{f(\mathbf{x})}$ is the variance of the evaluations of the benchmark function on the sampled points.

For each function, we generate 10 different datasets of 1000 points, each generated with a different randomly drawn covariance matrix. Therefore, for 7 global functions, we have 10 collections of input data, for a total of $7 \times 10 = 70$ datasets. This creates the first set of data.

For the second dataset, we follow the same procedure, but remove points surrounding the global optimal solution, to evaluate how well the PMO approaches can perform when the optimal value is far away from the training set. In particular, we generate 10 different datasets of 1500 points, each generated with a different randomly drawn covariance matrix, but now removing the data within a central region. This is described and evaluated in Section 4.4.

4.2 Predictive Modeling and Optimization Setup

For each dataset, we scale the independent variables to $[0, 1]$, standardize the dependent variable, and randomly split the dataset into a training set and a test set in the ratio of 7 : 3. Each training set is used to fit three different predictive models: linear regression, random forest, and neural networks, to be used in PMO.

For the configurations of the neurons in neural networks models, we consider a structure with two hidden layers. The number of neurons in each hidden layer ranges in $\{1, 2, \dots, 10\}$. For each dataset, we select the best neural networks model out of 500 candidates using the `GridSearchCV` function in **scikit-learn**. For random forest models, we create a hyper-parameters grid with the number of trees varying in $\{10, 20, \dots, 100\}$ and the maximum depth of the tree ranging in $\{1, 2, \dots, 10\}$. We try $10 \times 10 = 100$ combinations of parameters and select the best model using `GridSearchCV`. For linear regression models, we simply fit one single model using **scikit-learn** for each dataset.

The average out-of-sample performance, measured as R^2 , of the various predictive models are presented in Table 1. As we can see, the performance of linear regression is typically very poor for these functions due to the degree of nonlinearity, whereas random forest models and neural networks models have much better performance.

Table 1: Predictive models performances (R^2) for the test set of synthetic datasets

Predictive Model	Beale	Peaks	Griewank	Powell	Quintic	Qing	Rastrigin
Linear Regression	0.029	0.023	-0.009	-0.022	0.053	0.055	-0.017
Random Forest	0.305	0.445	0.416	0.360	0.390	0.390	0.152
Neural Networks	-0.298‡	0.435	0.396	0.393	0.376	0.374	0.071

‡ If a single outlier is removed, the R^2 is elevated to 0.297.

4.3 Optimization Results

Each predictive model fitted to each synthetic dataset is an instance. For each instance, we compare PMO with the following configurations:

- **BASE**: no constraints
- **IF**: IF constraints

- **SVM**: SVM constraints solved directly using BARON
- **SVM_{BC}**: SVM constraints solved with our heuristic branch-and-cut algorithm
- **CH**: CH constraints
- **PCA**: PCA constraints. We also run experiments with PCA as a penalty term, the same way as Mistry et al. [2021] propose. We omit these results as they are very similar to the ones reported modeling PCA via constraints.
- **MD**: MD constraints
- **KNN**: KNN constraints

For all the model formulations, as the input data is scaled between 0 and 1, the domain of the decision variables is $[0, 1]$. For **IF**, the isolation forest is pre-trained in Python using the **scikit-learn** package with all the hyperparameters setting as default. We set the tree depth threshold at $d = 5$ for datasets based on **Beale** and **Peaks**, and $d = 6$ for datasets based on **Griewank**, **Powell**, **Quintic**, **Qing**, and **Rastrigin**. We pick this parameter by approximately halving the average depth of training points across the trees. For **SVM**, we train the one-class SVM classifier using the **scikit-learn** package in Python. The hyperparameter γ is set as default in the training step. For **SVM_{BC}**, we set the number of pieces of the discretized ranges $m = 10$. For **PCA**, since the training datasets are not in high dimensions, we set the number of leading vectors $k = n - 1$ (n is the number of independent variables in the training datasets) to make sure that a subspace is defined and meanwhile it can explain the majority of the variance in the training data, and set $\gamma = 0.00001$. For **MD** we set significance level α at 0.05, i.e., $\gamma = \sqrt{\chi_{n,0.95}^2}$, as the input data follows a multivariate normal distribution. For **KNN**, we set $K = 1$ and $\gamma = 0.1n$. In a tuning process, we set $\beta = 10$ to only use the top 10% of the data (based on their value of their dependent variable) for formulating KNN constraints.

4.3.1 Solution Outcome Quality

We measure solution quality using two metrics: *true outcome* $f(\mathbf{x}^*)$ and *optimality error* $\Delta = |F(\mathbf{x}^*) - f(\mathbf{x}^*)|$, where \mathbf{x}^* denotes the optimal solution obtained via PMO. Table 2 reports the average improvement of solution quality for different PMO variants as compared to the **BASE** model over the 210 instances tested. Overall, **IF** is the best performer both in terms of true outcome and optimality error, followed by **SVM**.

Table 2: Improvement of solutions from PMO variant models in comparison with **BASE**

	$\frac{f(\mathbf{x}_{\text{BASE}}^*) - f(\mathbf{x}_{\text{variant}}^*)}{f(\mathbf{x}_{\text{BASE}}^*) - f(\mathbf{x}_{\text{min}})}$	$\frac{\Delta_{\text{BASE}} - \Delta_{\text{variant}}}{\Delta_{\text{BASE}}}$
IF	73.0%	81.6%
SVM	62.1%	75.2%
SVM_{BC}	64.3%	75.1%
CH	43.9%	49.9%
PCA	21.3%	23.3%
MD	46.2%	52.4%
KNN	58.2%	62.5%

Table 3 reports the average *true outcome* $f(\mathbf{x}^*)$ and the average *optimality error* Δ for the solutions obtained from the optimization models over all instances, grouped by benchmark function and predictive model. We also report the average true value $f(\mathbf{x})$ for the point in the training data with the smallest

observed outcome $y(\mathbf{x})$ in the training datasets, referred to as ‘Best Sample’. The best-performing model in each combination of benchmark function and predictive model are indicated in bold and underlined for *true outcome* and *optimality error*, respectively.

Table 3: Comparison $f(\mathbf{x}^*)$ from the optimization models for the benchmark functions using two metrics: average true outcome $f(\mathbf{x}^*)$ and average *optimality error* $\Delta = |F(\mathbf{x}^*) - f(\mathbf{x}^*)|$

		Beale		Peaks		Griewank		Powell		Quintic		Qing		Rastrigin	
		$f(\mathbf{x}^*)$	Δ	$f(\mathbf{x}^*)$	Δ	$f(\mathbf{x}^*)$	Δ	$f(\mathbf{x}^*)$	Δ	$f(\mathbf{x}^*)$	Δ	$f(\mathbf{x}^*)$	Δ	$f(\mathbf{x}^*)$	Δ
Linear Regression	BASE	3408	4980	0.00	2.98	1.04	0.68	30014	31967	3941	7804	1781	2931	260	210
	IF	8	293	-2.01	0.45	0.61	<u>0.02</u>	197	<u>278</u>	47	<u>224</u>	94	135	107	6
	SVM	3	257	-1.64	<u>0.02</u>	0.76	<u>0.17</u>	605	<u>621</u>	99	<u>1226</u>	80	323	115	22
	SVM_{BC}	3	<u>184</u>	-1.80	<u>0.27</u>	0.76	0.15	434	358	83	1029	75	<u>129</u>	106	3
	CH	635	<u>1940</u>	-0.07	2.30	1.01	0.42	4994	5002	2565	4411	1037	<u>1376</u>	119	17
	PCA	1683	3055	0.00	2.22	1.01	0.51	17540	18234	5234	7744	1699	2563	254	196
	MD	35	967	-0.17	1.93	0.89	0.29	4579	4633	2686	4761	1135	1606	130	34
	KNN	36	978	-0.69	1.25	0.54	0.07	680	653	584	1991	233	493	101	<u>1</u>
Random Forest	BASE	101	598	-6.03	0.76	0.44	0.23	689	1105	196	475	236	329	84	34
	IF	2	<u>52</u>	-6.16	0.91	0.09	0.17	30	<u>56</u>	63	<u>34</u>	51	<u>5</u>	58	10
	SVM	11	<u>155</u>	-6.03	0.76	0.19	0.06	206	<u>366</u>	76	<u>108</u>	179†	<u>138</u>	77†	7
	SVM_{BC}	24	168	-6.02	<u>0.75</u>	0.15	0.11	180	197	69	219	152	145	64	8
	CH	101	598	-6.03	<u>0.76</u>	0.38	0.15	490	824	138	411	135	204	68	13
	PCA	63	191	-6.35	1.09	0.39	0.18	591	913	232	505	233	317	74	23
	MD	26	350	-6.03	0.76	0.27	<u>0.04</u>	451	816	171	448	191	270	74	23
	KNN	34	452	-6.03	0.76	0.35	0.13	496	838	138	347	181	250	72	19
Neural Networks	BASE	2384	3050	-6.30	0.79	0.82	1.10	9026	11487	5069	7451	2226	2589	238	166
	IF	9	5	-6.32	0.46	0.13	<u>0.16</u>	107	<u>284</u>	81	<u>556</u>	48	<u>74</u>	121	27
	SVM	29	23	-6.30	0.79	0.36	<u>0.42</u>	280	<u>739</u>	56	<u>908</u>	108†	206	114†	20
	SVM_{BC}	13	3	-6.29	0.78	0.30	0.35	135	553	65	893	178†	219	105†	<u>8</u>
	CH	654	1109	-6.38	0.70	0.44	0.50	1015	1738	231	1255	132	216	102	10
	PCA	220	854	-6.44	<u>0.42</u>	0.43	0.60	3717	5145	5723	7248	2019	2352	211	137
	MD	56	395	-6.30	0.79	0.49	0.55	1137	2036	401	1489	138	262	124	37
	KNN	25	365	-6.36	0.73	0.16	0.19	624	1117	126	1066	101	173	85	9
Best Sample	2		-4.95		0.22		110		236		54		63		

† We are unable to obtain a feasible solution in 1, 4, 1, 3, 3, and 2 instances out of 10 instances within the time limit of 60 minutes for the combinations of **Qing** with random forest using **SVM**, **Rastrigin** with random forest using **SVM**, **Qing** with neural networks using **SVM** and **SVM_{BC}**, and **Rastrigin** with neural networks using **SVM** and **SVM_{BC}**, respectively.

We highlight several interesting observations. First and foremost, the quality of the solutions obtained through PMO is significantly better when trust-region constraints are added, independently of the predictive model chosen. Over the 210 instances tested, **BASE** achieves solutions better than the seven PMO variant models in 15, 38, 26, 36, 74, 36, 30 instances and is worse in 194, 172, 177, 146, 95, 159, 173 instances, respectively, for **IF**, **SVM**, **SVM_{BC}**, **CH**, **PCA**, **MD**, and **KNN**. From Table 3 we also see that **BASE** never achieves the best solution quality for any benchmark function and predictive model combination. This makes a clear case for why incorporating trust-region constraints is necessary in the context of PMO.

Furthermore, PMO variant models are more likely to identify solutions that are better than the best points in the training data, which suggests that the generalization of the predictive models is enhanced when solutions are constrained to a trust region. As an interesting example, for **Quintic** using linear regression, the average true outcome of the solutions obtained from **BASE** is 3,941, which is far away from the global minimum of 0. In comparison, **MD** improves the average true outcome to 2,686, **KNN** enhances the value to 584, **SVM** further pushes it to 99, and **IF** finds solutions closer to the global minimum with the average true outcome of 47.

IF delivers the most robust performance in terms of *true outcome* among all the models; it identifies the highest quality solution in average in 13 out of 21 combinations of benchmark function and predictive model. For the remaining eight scenarios, the performance of **IF** is marginally inferior to the best model. One can also infer from Table 2 and Table 3 that **SVM_{BC}** is the second best model tested. To compare the two best models, a detailed analysis between **IF** and **SVM_{BC}** grouped by the predictive models used in PMO is provided in Figure 4, in which three scatter plots comparing *true optimality gap* of solutions obtained from

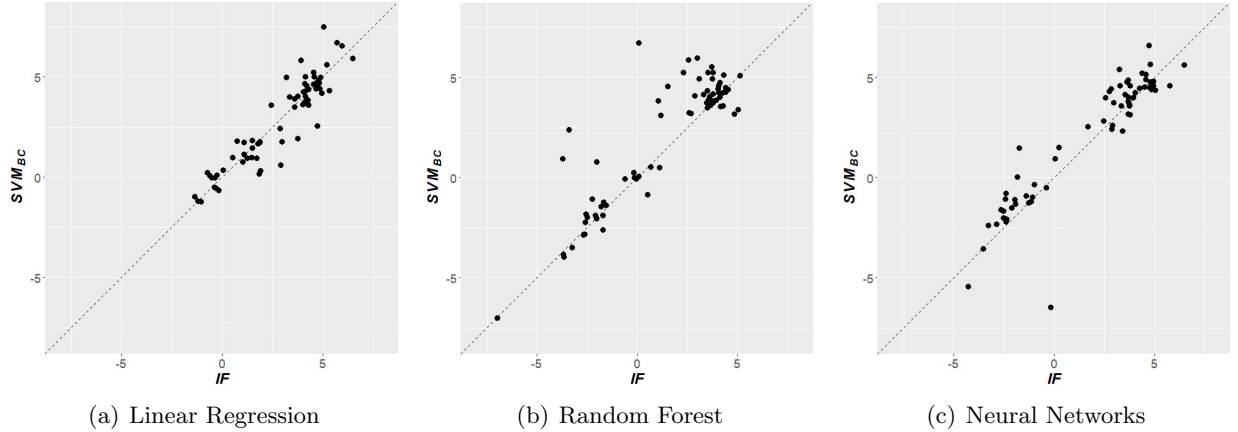


Figure 4: Scatter plots comparing the gap from true outcome to global minimum, $f(\mathbf{x}^*) - f(\mathbf{x}_{\min})$, between IF and SVM_{BC} based on different predictive models in natural logarithmic scale

IF and SVM_{BC} (calculated as $\log(f(\mathbf{x}^*) - f(\mathbf{x}_{\min}))$) are provided. Each point corresponds to an instance. A point above the dashed line at 45 degrees indicates that the true outcome of the solution obtained from IF is better than that from SVM_{BC} . When the predictive model is linear regression (Figure 4(a)), random forest (Figure 4(b)), and neural networks (Figure 4(c)), IF is better than SVM_{BC} in 36, 45, and 49 out of 70 instances, respectively.

Of note is that in Figure 4(a) we see that IF and SVM_{BC} have a similar performance when linear regression is employed as the predictive model. We hypothesize that the reason for such similar solution quality is the poor performance of linear regression in this setting (see Table 1). The performance difference between IF and SVM_{BC} is more obvious when the predictive model has higher performance. Figure 4(b) shows that with random forest as the predictive model the points tend to the bottom left corner and so are of better quality on average, but that the points deviate more from the 45 degrees dashed line in the vertical direction than in the horizontal direction, meaning that the *true optimality gap* from IF is much better than that from SVM_{BC} . An analogous pattern can be observed in Figure 4(c). Overall, Figure 4 clearly indicates the superiority of IF over the other tested models on the synthetic datasets. In addition, such dominance of IF can also be found in terms of the optimality error, which measures the level of overestimation at the solutions [Schweidtmann et al., 2022] and can be interpreted as the reliability of the solutions. According to Table 3, the performance of IF in terms of the optimality error is the most robust among all the models; it is the best among those models tested in 11 out of 21 scenarios. The overall improvement as compared to $BASE$, which is summarized in Table 2, also shows that IF is the best of all the PMO variant models.

A final takeaway is that MD and KNN are two alternative models worth exploration for any particular application. Although the performance of MD and KNN are unable to surpass SVM in terms of *true outcome*, both of them are better than PCA in 18 cases out of 21, and are better than CH in 9 cases and 16 cases out of 21, respectively. In addition, as summarized in Table 2, KNN ranks fourth place among the PMO variant models, only slightly worse than the best model in literature. Such good performance can also be supported by Table 3, through the results from **Rastrigin** in particular, which has 10 dimensions with the predictive model being linear regression and neural networks.

4.3.2 Computational Efficiency

From the results of solution outcome values reported in the Section 4.3.1, we observe that solutions from IF , SVM , and SVM_{BC} are significantly better than other PMO variant models, with IF being the best approach in terms of solution outcome quality.

Now we discuss the solution times for all models. Figure 5 shows a box plot of running time over all

10 instances using **Powell** as the benchmark function, with the three tested predictive models and the seven PMO variant models. Overall, Figure 5 highlights the computational efficiency of our **IF** model over the other models that achieve high-quality solutions based on SVMs. The running time of the majority of the instances using **MD**, **CH**, **KNN**, and **PCA**, and **IF** are within two seconds, but as discussed in the previous section, **IF** finds much better solutions. In contrast, the run time for **SVM** is significantly longer than other PMO variant models. For example, when the predictive model is linear regression, **SVM** uses nearly the full 60-minute time limit for all the 10 instances, among which only 2 instances are solved to optimality. Our implementation of **SVM_{BC}** improves the solution time of **SVM** significantly, but it still lags **IF** even for **Powell** which only has 4 dimensions.

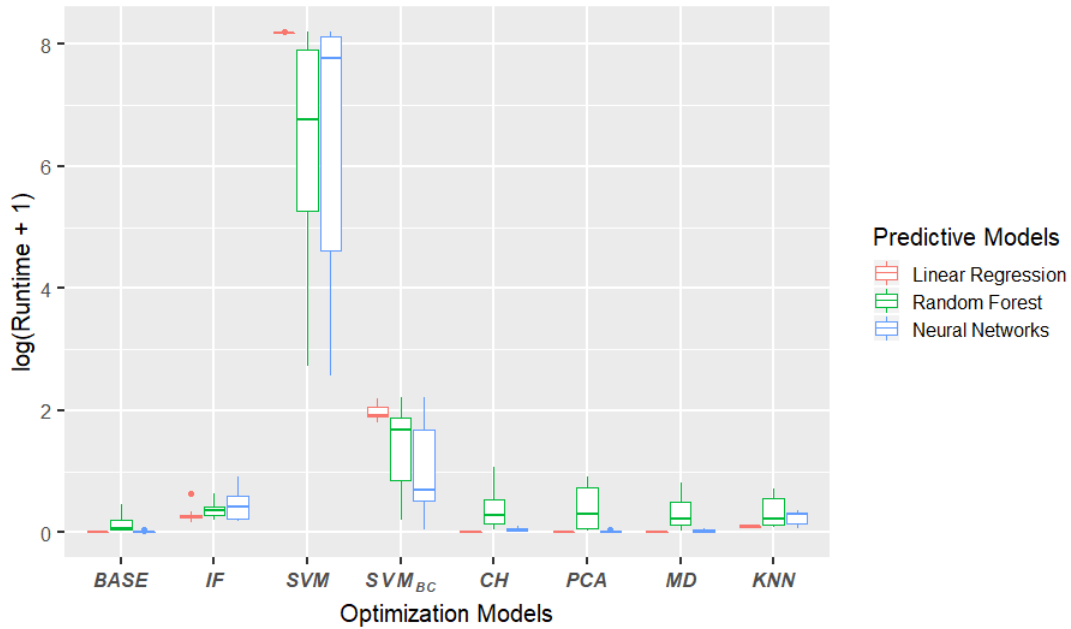


Figure 5: Solution times of instances generated with **Powell** and three predictive models using different optimization models in natural logarithmic scale

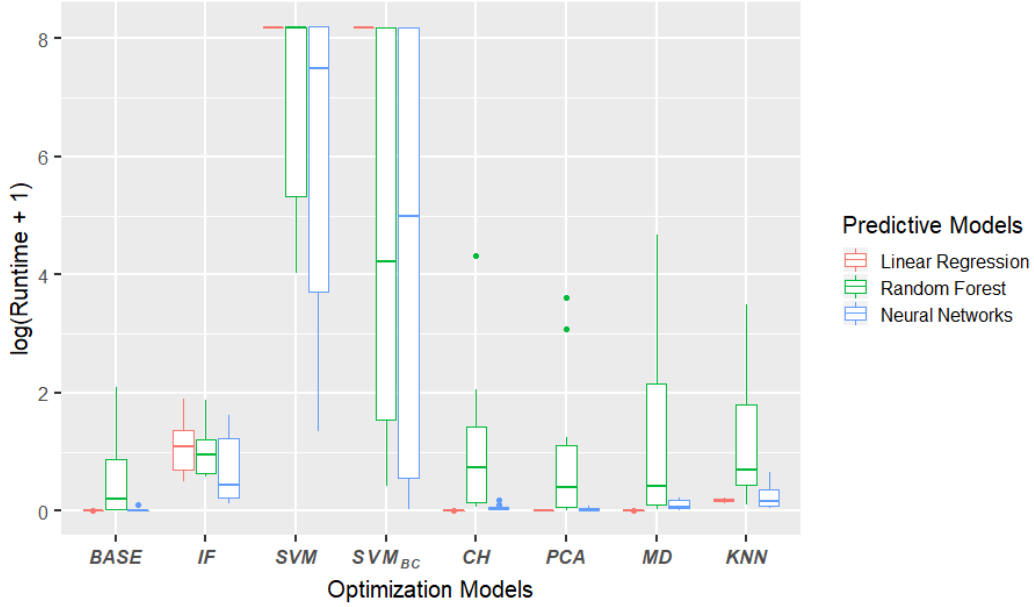


Figure 6: Solution times of instances generated with **Qing** and three predictive models using different optimization models in natural logarithmic scale

As expected, for the functions with more dimensions, the run time performance degrades. Figure 6 summarizes the runtimes for **Qing** function with 8 dimensions. Despite the overall increase in run time, we see that except *SVM* and *SVM_{BC}*, the **Qing** instances are solved within the time limit by all the remaining models, among which, *IF* exhibits a robust performance regardless of the predictive model. Appendix C summarizes the run time performance over all benchmark functions, which particularly highlight the robust computational performance of *IF*. We should note that, for **Rastrigin** function, computational times across all constraint types for the random forest model are higher. This is mainly due to the instance complexities for the random forest-based PMO model even without any trust-region constraint.

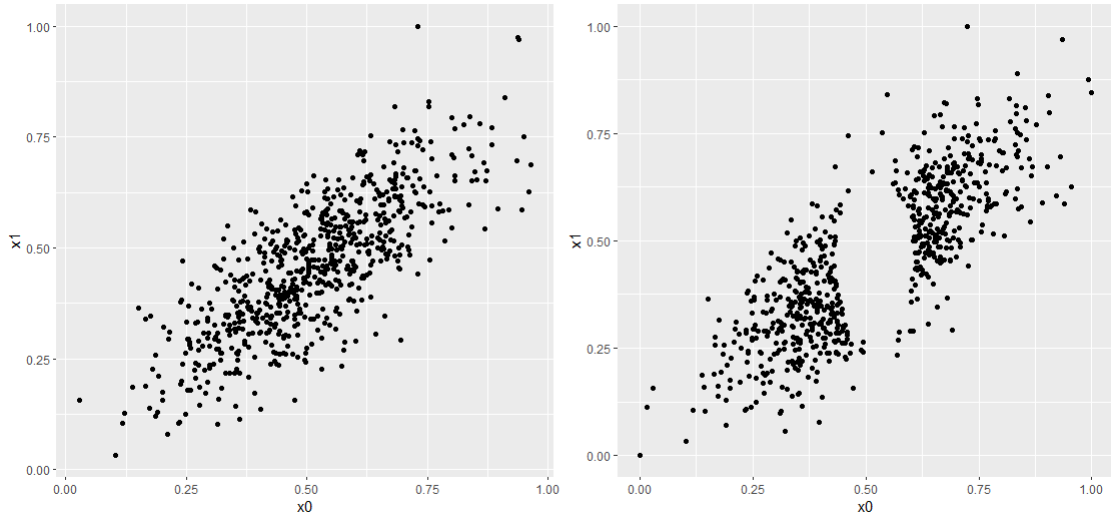


Figure 7: Comparison of shapes of datasets simulated with **Peaks** function using same parameter setting, with the left figure depicting the first experimental setting and the right figure showing the result of removing points in the optimum.

4.4 Robustness Check: Sampling Away from Global Optimum

In addition to the experimental results from the 70 synthetic datasets, we also run a similar experiment on another 70 synthetic datasets by taking a different random sampling approach. To be more specific, in these datasets we exclude the samples in the neighborhood of the global optimum. With the same seven benchmark functions, we first generate 1500 sample points instead of 1000 sample points for each dataset using the same sampling procedure in Section 4.1. We then create a hole centering at the global optimum of the benchmark function with radius $r = \frac{1}{2}\sqrt{\sigma_1^2 + \dots + \sigma_n^2}$, where σ_i^2 is the variance of independent variable x_i and is obtained from the randomly generated covariance matrix. Finally, we remove sample points falling within the radius. Figure 7 illustrates the shapes of two datasets simulated using **Peaks** function.

Table 4: Comparison $f(\mathbf{x}^*)$ from the optimization models for the benchmark functions using two metrics: average true outcome $f(\mathbf{x}^*)$ and average *optimality error* $\Delta = |F(\mathbf{x}^*) - f(\mathbf{x}^*)|$

		Beale		Peaks		Griewank		Powell		Quintic		Qing		Rastrigin	
		$f(\mathbf{x}^*)$	Δ	$f(\mathbf{x}^*)$	Δ	$f(\mathbf{x}^*)$	Δ	$f(\mathbf{x}^*)$	Δ	$f(\mathbf{x}^*)$	Δ	$f(\mathbf{x}^*)$	Δ	$f(\mathbf{x}^*)$	Δ
Linear Regression	BASE	9375	11320	0.00	2.16	1.03	0.48	16121	17009	3835	7623	1992	3507	278	223
	IF	11	367	-0.39	0.14	0.61	<u>0.18</u>	194	584	68	<u>411</u>	81	151	108	<u>3</u>
	SVM	8	444	-0.85	<u>0.10</u>	0.96	<u>0.23</u>	667	251	116	<u>1190</u>	118	578	118	22
	SVM_{BC}	4	<u>172</u>	-0.72	<u>0.15</u>	0.90	0.17	603	<u>113</u>	102	1044	61	<u>128</u>	113	9
	CH	581	2170	-0.02	1.35	0.92	0.20	7230	<u>7074</u>	3005	5008	1045	<u>1415</u>	142	36
	PCA	1546	3184	0.00	1.07	1.04	0.42	15585	15975	5369	8206	2301	3370	267	194
	MD	66	1383	-0.03	1.13	0.93	0.21	13355	13278	3770	6024	1260	1756	126	24
	KNN	36	1434	-0.25	0.94	0.74	<u>0.01</u>	1575	1197	1552	3095	265	586	110	6
Random Forest	BASE	53	627	-2.39	0.04	0.48	0.23	502	1069	250	326	254	255	84	25
	IF	15	<u>38</u>	-1.92	0.10	0.23	0.18	115	<u>125</u>	95	48	54	<u>7</u>	60	21
	SVM	80	152	-2.29	0.29	0.30	<u>0.10</u>	219	450	113	<u>13</u>	109§	40	91§	17
	SVM_{BC}	16	83	-2.63	0.64	0.26	<u>0.14</u>	198	377	119	<u>16</u>	90	72	55	12
	CH	27	558	-2.42	<u>0.02</u>	0.46	0.20	577	1085	118	123	157	148	67	<u>1</u>
	PCA	265	643	-4.57	<u>2.55</u>	0.54	0.26	842	1313	285	355	215	211	84	24
	MD	154	553	-2.48	0.16	0.40	.12	750	1261	232	252	163	158	75	16
	KNN	39	536	-2.24	0.20	0.44	0.18	458	944	152	128	147	131	65	3
Neural Networks	BASE	8713	9179	-0.99	5.15	1.03	1.47	5059	6742	3789	5714	2273	2802	262	190
	IF	5	104	-3.76	0.59	0.18	<u>0.03</u>	162	<u>291</u>	148	<u>204</u>	63	<u>155</u>	111	12
	SVM	9	133	-3.55	<u>0.34</u>	0.47	<u>0.37</u>	409	792	309	483	92	<u>274</u>	107§	7
	SVM_{BC}	12	<u>89</u>	-3.66	<u>0.47</u>	0.38	0.27	324	653	187	504	73	226	101	<u>1</u>
	CH	406	703	-2.53	1.35	0.40	0.36	789	1320	216	814	222	352	106	9
	PCA	1038	1214	-3.88	0.65	0.94	1.04	2708	4094	2547	3851	1285	1658	228	151
	MD	138	387	-2.99	0.55	0.51	0.50	911	1374	267	1012	120	291	103	12
	KNN	157	407	-2.36	0.84	0.30	0.27	358	870	170	652	144	263	100	6
Best Sample	34		-1.91		0.31		334		283		158		69		

§ We are unable to obtain a feasible solution in 1, 7, and 3 instances out of 10 within the time limit of 60 minutes for the combinations of **Qing** with random forest using **SVM**, **Rastrigin** with random forest using **SVM_{BC}**, and **Rastrigin** with neural networks using **SVM_{BC}**, respectively.

Similar to the pattern that we observe in Table 3, Table 4 exhibits the dominance of **IF** among all the PMO variant models; it provides the best solution in terms of *true outcome* in 14 cases out of 21. **IF** also is the best in terms of *optimality error*.

5 Conclusions and Future Work

In this paper, we investigate seven PMO variant models with constraints describing a trust region. We assess the performance of both the constraints existing in literature and our proposed constraints, validate the importance of considering a trust region, and highlight that constraints learned from isolation forests outperform existing approaches in both solution quality and computational performance through extensive experimentation on several synthetic datasets.

Among the existing approaches, one-class SVM constraints work best in terms of solution quality but

impose a high computational burden to the PMO models. In addition to isolation forest, we explore two other common outlier detection methods, Mahalanobis distance and K -nearest neighbors. The performance of trust-region constraints based on these two methods is better than two other existing approaches, namely, convex hull constraints and PCA constraints.

There is a wide array of research that can expand on the work in this paper, including the following. First, we do not investigate specific algorithms well suited for each predictive model and each PMO variant model. We observed that **SVM** suffers from the complexity brought by the exponential constraints. Trust-region constraints in other PMO variant models could also potentially significantly increase the solution times (e.g., consider the auxiliary binary variables and big-M constraints for **KNN**). Advanced optimization algorithms and stronger formulations may be applicable to greatly improve computational times. Second, an investigation of which type of trust-region constraint to add for different contexts is important. We show that adding trust-region constraints nearly always leads to higher quality solutions in our experiments, but using different constraints results in varied solution quality and understanding this connection would make the decision-making pipeline more robust. Third, we explored three classes of trust-region constraints based on existing outlier detection methods. There are a variety of additional methods from the literature of outlier detection, which can be used for characterizing a trust region and could offer different tradeoffs between solution quality and computational performance.

References

- Naomi S Altman. An introduction to kernel and nearest-neighbor nonparametric regression. *The American Statistician*, 46(3):175–185, 1992.
- Dario Amodei, Chris Olah, Jacob Steinhardt, Paul Christiano, John Schulman, and Dan Mané. Concrete problems in ai safety. *arXiv preprint arXiv:1606.06565*, 2016.
- Ross Anderson, Joey Huchette, Will Ma, Christian Tjandraatmadja, and Juan Pablo Vielma. Strong mixed-integer programming formulations for trained neural networks. *Mathematical Programming*, pages 1–37, 2020.
- Lennart Baardman, Maxime C Cohen, Kiran Panchangam, Georgia Perakis, and Danny Segev. Scheduling promotion vehicles to boost profits. *Management Science*, 65(1):50–70, 2019.
- David Bergman, Teng Huang, Philip Brooks, Andrea Lodi, and Arvind U Raghunathan. Janos: an integrated predictive and prescriptive modeling framework. *INFORMS Journal on Computing*, 34(2):807–816, 2022.
- Dimitris Bertsimas, Allison O’Hair, Stephen Relyea, and John Silberholz. An analytics approach to designing combination chemotherapy regimens for cancer. *Management Science*, 62(5):1511–1531, 2016.
- Max Biggs, Rim Hariss, and Georgia Perakis. Optimizing objective functions determined from random forests. *Available at SSRN 2986630*, 2017.
- Max Biggs, Wei Sun, and Markus Ettl. Model distillation for revenue optimization: Interpretable personalized pricing. In *International Conference on Machine Learning*, pages 946–956. PMLR, 2021.
- Elena Botoeva, Panagiotis Kouvaros, Jan Kronqvist, Alessio Lomuscio, and Ruth Misener. Efficient Verification of ReLU-Based Neural Networks via Dependency Analysis. *Proceedings of the AAAI Conference on Artificial Intelligence*, 34(04):3291–3299, April 2020. ISSN 2374-3468, 2159-5399. doi: 10.1609/aaai.v34i04.5729. URL <https://aaai.org/ojs/index.php/AAAI/article/view/5729>.
- Rudy Bunel, Ilker Turkaslan, Philip H. S. Torr, Pushmeet Kohli, and M. Pawan Kumar. A Unified View of Piecewise Linear Neural Network Verification. *arXiv:1711.00455 [cs]*, May 2018. URL <http://arxiv.org/abs/1711.00455>. arXiv: 1711.00455.
- Chih-Hong Cheng, Georg Nührenberg, and Harald Ruess. Maximum resilience of artificial neural networks. In *International Symposium on Automated Technology for Verification and Analysis*, pages 251–268. Springer, 2017.

- Souradeep Dutta, Susmit Jha, Sriram Sankaranarayanan, and Ashish Tiwari. Output range analysis for deep feedforward neural networks. In *NASA Formal Methods Symposium*, pages 121–138. Springer, 2018.
- Kris Johnson Ferreira, Bin Hong Alex Lee, and David Simchi-Levi. Analytics for an online retailer: Demand forecasting and price optimization. *Manufacturing & Service Operations Management*, 18(1):69–88, 2016.
- Matteo Fischetti and Jason Jo. Deep neural networks and mixed integer linear optimization. *Constraints*, 23(3):296–309, 2018.
- Jerome H Friedman. *The elements of statistical learning: Data mining, inference, and prediction*. springer open, 2017.
- Andrea Gavana. Index of test functions in global optimization problems, 2022. http://infinity77.net/global_optimization/test_functions.html#multidimensional-test-functions-index, Last accessed on 2022-10-03.
- Bjarne Grimstad and Henrik Andersson. Relu networks as surrogate models in mixed-integer linear programs. *Computers & Chemical Engineering*, 131:106580, 2019a.
- Bjarne Grimstad and Henrik Andersson. ReLU networks as surrogate models in mixed-integer linear programs. *Computers & Chemical Engineering*, 131:106580, December 2019b. ISSN 00981354. doi: 10.1016/j.compchemeng.2019.106580.
- Gurobi Optimization LLC. Gurobi optimizer reference manual, 2020. <https://www.gurobi.com>.
- Thomas Hofmann, Bernhard Schölkopf, and Alexander J Smola. Kernel methods in machine learning. *The annals of statistics*, 36(3):1171–1220, 2008.
- Teng Huang, David Bergman, and Ram Gopal. Predictive and prescriptive analytics for location selection of add-on retail products. *Production and Operations Management*, 28(7):1858–1877, 2019.
- Richard Arnold Johnson, Dean W Wichern, et al. *Applied multivariate statistical analysis*, volume 6. Pearson London, UK:, 2014.
- Ian T Jolliffe. *Principal component analysis for special types of data*. Springer, 2002.
- Guy Katz, Clark Barrett, David L Dill, Kyle Julian, and Mykel J Kochenderfer. Reluplex: An efficient smt solver for verifying deep neural networks. In *International Conference on Computer Aided Verification*, pages 97–117. Springer, 2017.
- Christophe Leys, Olivier Klein, Yves Dominicy, and Christophe Ley. Detecting multivariate outliers: Use a robust variant of the mahalanobis distance. *Journal of Experimental Social Psychology*, 74:150–156, 2018.
- Fei Tony Liu, Kai Ming Ting, and Zhi-Hua Zhou. Isolation forest. In *2008 Eighth IEEE International Conference on Data Mining*, pages 413–422. IEEE, 2008.
- Sheng Liu, Long He, and Zuo-Jun Max Shen. On-Time Last-Mile Delivery: Order Assignment with Travel-Time Predictors. *Management Science*, November 2020. ISSN 0025-1909. <https://pubsonline.informms.org/doi/abs/10.1287/mnsc.2020.3741>.
- Alessio Lomuscio and Lalit Maganti. An approach to reachability analysis for feed-forward ReLU neural networks. *arXiv:1706.07351 [cs]*, June 2017. <http://arxiv.org/abs/1706.07351>.
- Prasanta Chandra Mahalanobis. On the generalized distance in statistics. National Institute of Science of India, 1936.
- Donato Maragno, Holly Wiberg, Dimitris Bertsimas, S Ilker Birbil, Dick den Hertog, and Adejuyigbe Fajemisin. Mixed-integer optimization with constraint learning. *arXiv preprint arXiv:2111.04469*, 2021.

- Velibor V Mišić. Optimization of tree ensembles. *Operations Research*, 68(5):1605–1624, 2020.
- Miten Mistry, Dimitrios Letsios, Gerhard Krennrich, Robert M Lee, and Ruth Misener. Mixed-integer convex nonlinear optimization with gradient-boosted trees embedded. *INFORMS Journal on Computing*, 33(3):1103–1119, 2021.
- Ioulia Papageorgiou. Ceramic investigation: how to perform statistical analyses. *Archaeological and Anthropological Sciences*, 12(9):1–19, 2020.
- F. Pedregosa, G. Varoquaux, A. Gramfort, V. Michel, B. Thirion, O. Grisel, M. Blondel, P. Prettenhofer, R. Weiss, V. Dubourg, J. Vanderplas, A. Passos, D. Cournapeau, M. Brucher, M. Perrot, and E. Duchesnay. Scikit-learn: Machine learning in Python. *Journal of Machine Learning Research*, 12:2825–2830, 2011.
- N. V. Sahinidis. *BARON 21.1.13: Global Optimization of Mixed-Integer Nonlinear Programs*, User’s Manual, 2017.
- Bernhard Schölkopf, Robert C Williamson, Alex Smola, John Shawe-Taylor, and John Platt. Support vector method for novelty detection. *Advances in neural information processing systems*, 12, 1999.
- Artur M Schweidtmann and Alexander Mitsos. Deterministic global optimization with artificial neural networks embedded. *Journal of Optimization Theory and Applications*, 180(3):925–948, 2019.
- Artur M Schweidtmann, Jana M Weber, Christian Wende, Linus Netze, and Alexander Mitsos. Obey validity limits of data-driven models through topological data analysis and one-class classification. *Optimization and Engineering*, 23(2):855–876, 2022.
- Thiago Serra, Christian Tjandraatmadja, and Srikumar Ramalingam. Bounding and counting linear regions of deep neural networks. In *International Conference on Machine Learning*, pages 4558–4566. PMLR, 2018.
- DMJ Tax. One class classification: Concept learning in the absence of counter examples [ph. d dissertation]. *Netherlands Delft University of Technology. Faculty of Information Technologand Systems*, 2001.
- Ana P Teixeira, João J Clemente, António E Cunha, Manuel JT Carrondo, and Rui Oliveira. Bioprocess iterative batch-to-batch optimization based on hybrid parametric/nonparametric models. *Biotechnology progress*, 22(1):247–258, 2006.
- The MathWorks Inc. peaks minimization with globalsearch, 2010. <https://www.mathworks.com/matlabcentral/mlc-downloads/downloads/submissions/27178/versions/6/previews/html/gspEaksExample.html>, Last accessed on 2022-10-03.
- Vincent Tjeng, Kai Xiao, and Russ Tedrake. Evaluating Robustness of Neural Networks with Mixed Integer Programming. *arXiv:1711.07356 [cs]*, February 2019. <http://arxiv.org/abs/1711.07356>.
- Calvin Tsay, Jan Kronqvist, Alexander Thebelt, and Ruth Misener. Partition-based formulations for mixed-integer optimization of trained relu neural networks. *arXiv preprint arXiv:2102.04373*, 2021.
- Sicco Verwer, Yingqian Zhang, and Qing Chuan Ye. Auction optimization using regression trees and linear models as integer programs. *Artificial Intelligence*, 244:368–395, 2017.
- Keliang Wang, Leonardo Lozano, David Bergman, and Carlos Cardonha. A two-stage exact algorithm for optimization of neural network ensemble. In *International Conference on Integration of Constraint Programming, Artificial Intelligence, and Operations Research*, pages 106–114. Springer, 2021.
- Shuo Zheng, Yu-Xin Zhu, Dian-Qing Li, Zi-Jun Cao, Qin-Xuan Deng, and Kok-Kwang Phoon. Probabilistic outlier detection for sparse multivariate geotechnical site investigation data using bayesian learning. *Geoscience Frontiers*, 12(1):425–439, 2021.

Appendix A PMO Formulations with Different Predictive Models

A.1 Linear Regression-based PMO Formulation

For a linear regression model, the objective function can be expressed as $F(\mathbf{x}) = b_0 + b_1x_1 + \dots + b_nx_n$. As a result, the PMO formulation is given by the following linear program:

$$\min_{\mathbf{x}} \quad b_0 + b_1x_1 + \dots + b_nx_n \quad (\text{A.1a})$$

$$\text{s.t.} \quad \mathbf{x} \in [0, 1]. \quad (\text{A.1b})$$

A.2 Random Forest-based PMO Formulation

A.2.1 Background on Random Forests

We consider random forest regression models in this paper, where the outcome variable is continuous. Let \mathcal{T}^{RF} be the index set of trees in the random forest. Each tree $t \in \mathcal{T}^{\text{RF}}$ has the same weight in the prediction and is trained over a randomly selected subsample of the training data. Similar to isolation trees, the prediction for an observation is determined by checking a series of splits. Each leaf node ℓ from tree $t \in \mathcal{T}^{\text{RF}}$ has a score $\mathbf{p}_{t,\ell}$. Any vector of independent variables \mathbf{x} corresponds to a leaf node of the tree, denoted by $\ell(\mathbf{x})$. The predicted outcome for an input vector \mathbf{x} from tree t is given by the corresponding score $\mathbf{p}_{t,\ell(\mathbf{x})}$. As a result, the prediction of the random forest for a given \mathbf{x} is given by the average of the corresponding scores:

$$F(\mathbf{x}) = \frac{1}{|\mathcal{T}^{\text{RF}}|} \sum_{t \in \mathcal{T}^{\text{RF}}} \mathbf{p}_{t,\ell(\mathbf{x})}$$

A.2.2 Optimization Model

Inspired by Mišić [2020], we present a PMO formulation to solve optimization problems over a pre-trained random forest. The objective of the optimization problem is to find the independent variable vector \mathbf{x} that minimizes the outcome predicted by the random forest $F(\mathbf{x})$. This can be casted as the problem of finding a leaf node from each tree in the random forest that minimize the average outcome.

Consider a random forest with $|\mathcal{T}^{\text{RF}}|$ trees. Let $\mathcal{L}_t^{\text{RF}}$ be the set of leaf nodes in tree $t \in \mathcal{T}^{\text{RF}}$. We introduce binary decision variable $y_{t,\ell}$ that takes a value of 1 if leaf node ℓ from tree $t \in \mathcal{T}^{\text{RF}}$ is selected. We introduce auxiliary decision variables (\mathbf{z}_i^{LB} , \mathbf{z}_i^{UB}) to specify the range of each variable feature $i \in \mathcal{I}$. Let the lower and upper bounds corresponding to a leaf node be $l_{i,t,\ell}^{\text{RF}}$ and $u_{i,t,\ell}^{\text{RF}}$ for all $i \in \mathcal{I}$, $t \in \mathcal{T}^{\text{RF}}$, and $\ell \in \mathcal{L}_t^{\text{RF}}$. Our formulation of the random forest-based optimization problem is:

$$\min_{\mathbf{x}, \mathbf{y}, \mathbf{z}} \quad \frac{1}{|\mathcal{T}^{\text{RF}}|} \sum_{t \in \mathcal{T}^{\text{RF}}} \sum_{\ell \in \mathcal{L}_t^{\text{RF}}} \mathbf{p}_{t,\ell} \mathbf{y}_{t,\ell} \quad (\text{A.2a})$$

$$\text{s.t.} \quad \sum_{\ell \in \mathcal{L}_t^{\text{RF}}} y_{t,\ell} = 1 \quad \forall t \in \mathcal{T}^{\text{RF}} \quad (\text{A.2b})$$

$$\sum_{\ell \in \mathcal{L}_t^{\text{RF}}} l_{i,t,\ell}^{\text{RF}} y_{t,\ell} \leq \mathbf{z}_i^{LB} \quad \forall t \in \mathcal{T}^{\text{RF}}, \forall i \in \mathcal{I} \quad (\text{A.2c})$$

$$1 - \sum_{\ell \in \mathcal{L}_t^{\text{RF}}} (1 - u_{i,t,\ell}^{\text{RF}}) y_{t,\ell} \geq \mathbf{z}_i^{UB} \quad \forall t \in \mathcal{T}^{\text{RF}}, \forall i \in \mathcal{I} \quad (\text{A.2d})$$

$$\mathbf{z}_i^{LB} \leq x_i \leq \mathbf{z}_i^{UB} - \epsilon \quad \forall i \in \mathcal{I} \quad (\text{A.2e})$$

$$x_i, \mathbf{z}_i^{LB}, \mathbf{z}_i^{UB} \in [0, 1] \quad \forall i \in \mathcal{I} \quad (\text{A.2f})$$

$$y_{t,\ell} \in \{0, 1\} \quad \forall t \in \mathcal{T}^{\text{RF}}, \ell \in \mathcal{L}_t^{\text{RF}} \quad (\text{A.2g})$$

Constraints (A.2b) ensure that exactly one of the leaf nodes from each tree in the random forest is selected. Constraints (A.2c) and constraints (A.2d) ensure that, for any leaf node that is selected, the domain of the solution is limited to the feature ranges determined by the path leading to that leaf node. Constraints (A.2e) ensure that \mathbf{x} belongs to the domain defined by the corresponding leaf nodes selected.

A.3 Neural Networks-based PMO Formulation

There is plenty of literature on formulating neural networks models as a mixed integer programming problem. In particular, we make use of recent work that solve the neural networks-based optimization problem. For the details of the formulation, the reader is referred to Bergman et al. [2022].

Appendix B Details of the Branch-and-Cut Algorithm for PMO Model with One-Class SVM Constraints

Recall that $\mathbf{x} = \{x_i\}_{i=1}^n$ are the main decision variables in a PMO model, determining the value of each feature $i \in \mathcal{I}$. For the branch-and-cut algorithm, we first discretize the range of each feature $i \in \mathcal{I}$ into m pieces. As each feature is scaled to $[0,1]$, the m pieces of the discretized ranges for each feature are $[0, \frac{1}{m}]$, $[\frac{1}{m} + \epsilon, \frac{2}{m}]$, $[\frac{2}{m} + \epsilon, \frac{3}{m}]$, ..., $[\frac{m-1}{m} + \epsilon, \frac{m}{m}]$, where ϵ is a small number (we set $\epsilon = \frac{1}{10m}$). Binary decision variable $v_{i,p}$ equals 1, if the value of feature $i \in \mathcal{I}$ falls into range $p \in \mathcal{P} = \{1, 2, \dots, m\}$. The master problem is formulated on the basis of PMO model (1a) with additional constraints connecting decision variables \mathbf{x} and $v_{i,p}$:

$$0 \leq x_i \leq \frac{1}{m} + 1 - v_{i,1} \quad \forall i \in \mathcal{I} \quad (\text{B.1})$$

$$\left(\frac{p-1}{m} + \epsilon\right)v_{i,p} \leq x_i \leq \frac{p}{m} + 1 - v_{i,p} \quad \forall i \in \mathcal{I}, \forall p \in \mathcal{P} \text{ and } p \geq 2 \quad (\text{B.2})$$

$$\sum_{p \in \mathcal{P}} v_{i,p} = 1 \quad \forall i \in \mathcal{I} \quad (\text{B.3})$$

$$v_{i,p} \in \{0, 1\} \quad \forall i \in \mathcal{I}, \forall p \in \mathcal{P} \quad (\text{B.4})$$

We describe the procedure of our proposed branch-and-cut algorithm in Algorithm 1 and note that this branch-and-cut algorithm is a heuristic. The algorithm can be implemented using a call-back function by dynamically checking sub-problem constraints for integer nodes, and adding cuts while the branch-and-bound tree is being built.

Algorithm 1 The Branch-and Cut Procedure for PMO with One-Class SVM Constraints

Candidate solution $(\bar{\mathbf{x}}, \bar{\mathbf{v}}) \leftarrow$ solve PMO (1a) with constraints B.1-B.4

if $\bar{\mathbf{x}}$ violates SVM constraints 4 **then**

Add a cover cut $\sum_{i \in \mathcal{I}} \sum_{p \in \mathcal{P}: \bar{v}_{i,p}=1} v_{i,p} \leq n - 1$

else

return $\bar{\mathbf{x}}$ as the final solution

Note that the cover cuts ensure that any given combination of the discretization ranges is explored at most once during the execution of the algorithm. The algorithm terminates in a finite number of steps because there is a finite number of combinations for the discretization ranges.

Appendix C Running Time Summary of Each Benchmark Function

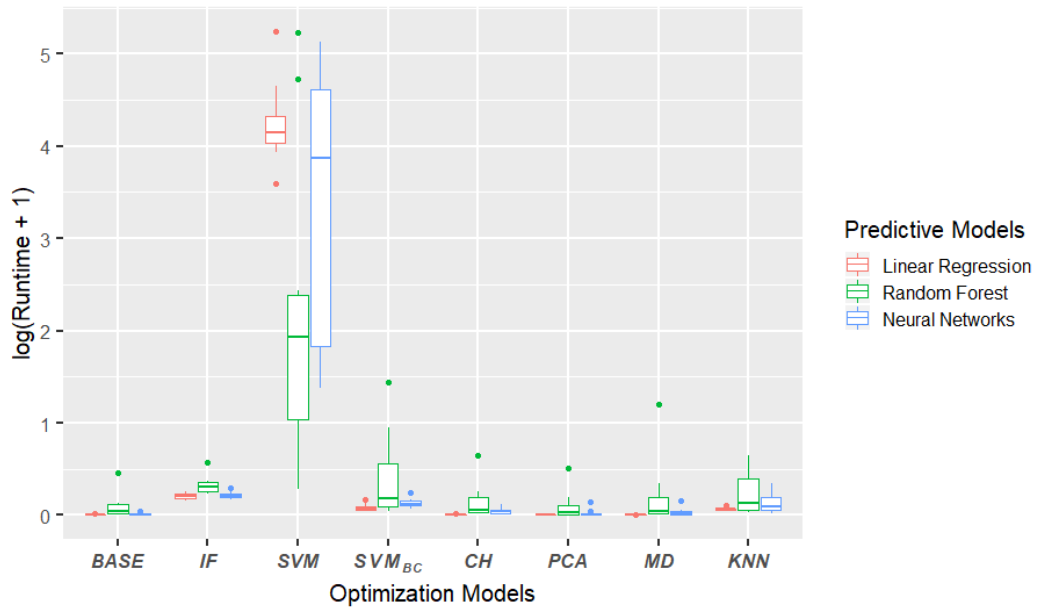


Figure 8: Solution times of instances generated with **Beale** and three predictive models using different optimization models in natural logarithmic scale



Figure 9: Solution times of instances generated with **Peaks** and three predictive models using different optimization models in natural logarithmic scale

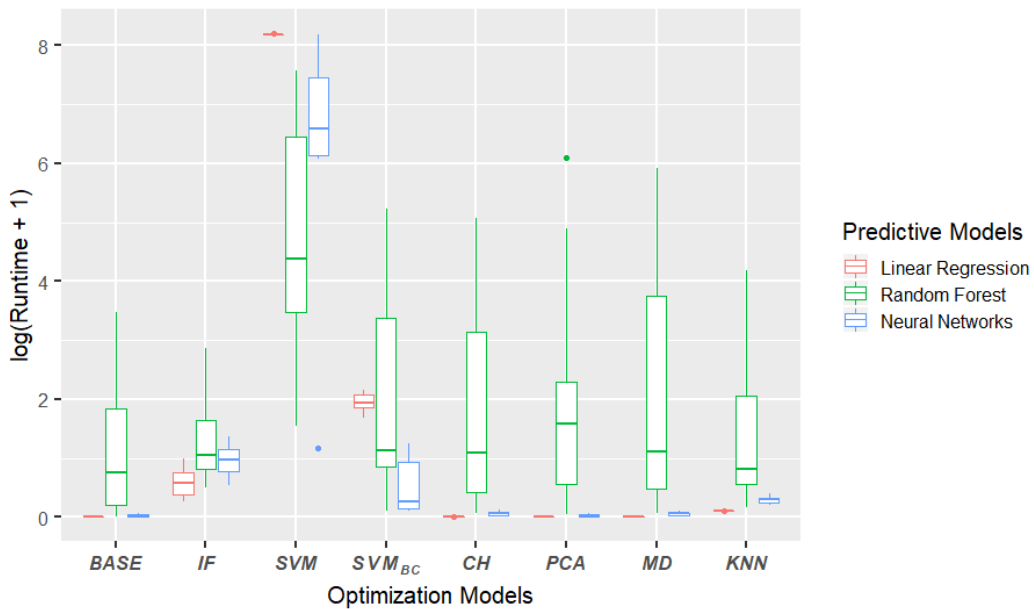


Figure 10: Solution times of instances generated with **Griewank** and three predictive models using different optimization models in natural logarithmic scale

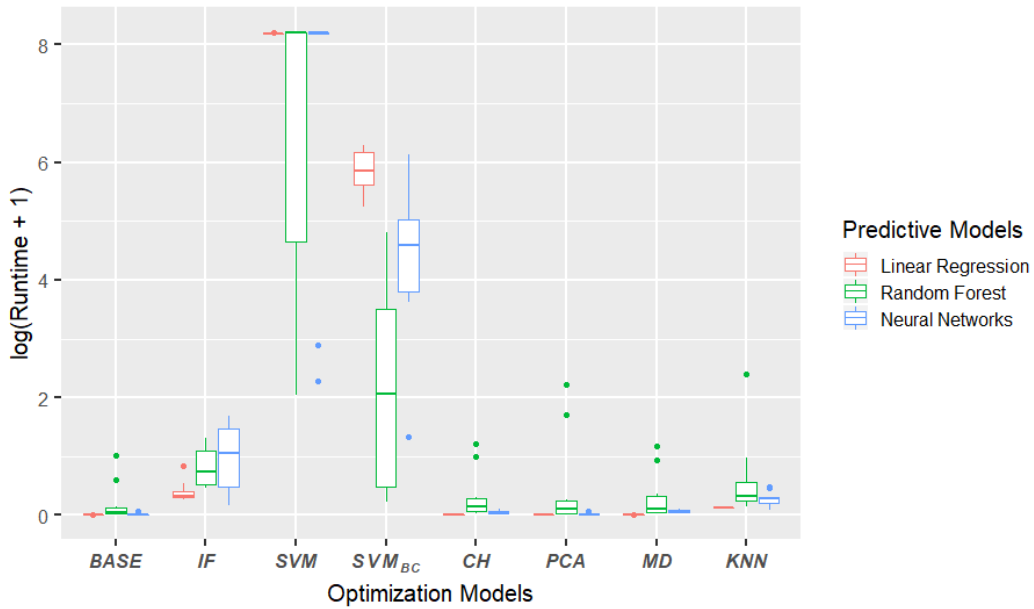


Figure 11: Solution times of instances generated with **Quintic** and three predictive models using different optimization models in natural logarithmic scale

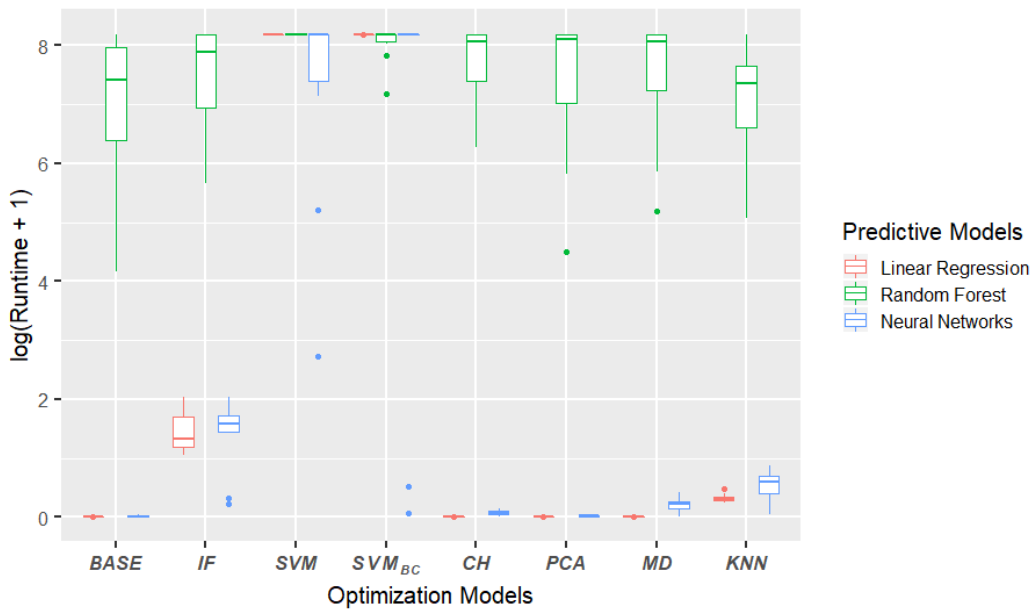


Figure 12: Solution times of instances generated with **Rastrigin** and three predictive models using different optimization models in natural logarithmic scale